

**104-Plat****Load Dependence of the Degree of Cooperativity of the Unwinding of Dna Helix**Pasquale Bianco<sup>1,2</sup>, Mario Dolfi<sup>1</sup>, Vincenzo Lombardi<sup>1,2</sup>.<sup>1</sup>University of Florence, Florence, Italy, <sup>2</sup>CRS-SOFT, INFM-CNR, Rome, Italy.

We use a dual-laser optical-tweezers (DLOT, Smith et al., *Science*, 271:795, 1996) to define the highly cooperative conformational transition in the molecule of DNA, where the natural B-DNA is converted into a new overstretched conformation called S-DNA (Bensimon et al., *Phys. Rev. Lett.* **74**, 4754, 1995; Cluzel et al., *Science* **271**, 792, 1996). Single molecules of double stranded  $\lambda$ -phage DNA are stretched at 27 °C with the DLOT either with ramp length changes or with force step staircases. The microchamber solution contains 150 mM NaCl, 10 mM tris-HCl, 1 mM EDTA, pH 8.0. When the DNA molecule is stretched in length clamp mode, it shows the previously described highly cooperative overstretching transition at ~60 pN, attributed to unwinding from the B-form to the 1.7 times longer S-form. Stretching the molecule in force clamp mode with a staircase of force steps ( $\Delta F$ , step size 1-5 pN) at 5 s intervals shows different amount of DNA elongation ( $\Delta L$ ) for a given clamped force  $F$  depending on  $\Delta F$ . The peak of the Gaussian fit to the  $\Delta L$ - $F$  relations is at ~60 pN independently of the step size, but the  $\sigma$  of the Gaussian is smaller at smaller  $\Delta F$ . The  $L$ - $F$  relations obtained by integrating the Gaussian curves, fitted with the Hill sigmoid equation, show a Hill coefficient  $n$  (an estimate of the order of the underlying transition) that increases with the reduction of  $\Delta F$ .  $n$  is 20, 70 and 125 with  $\Delta F = 5, 2$  and 1 pN respectively. These results demonstrate the importance of fine force clamp to establish the degree of bps cooperativity for the unwinding of DNA helix. Supported by MiUR, Ente Cassa di Risparmio di Firenze (2007. 1421) and ITB-CNR (Milano).

**105-Plat****Unraveling the Structure of a Single DNA During Overstretching Using Multicolor Fluorescence Imaging**Peter Gross<sup>1</sup>, Joost van Mameren<sup>1</sup>, Geraldine Farge<sup>1</sup>, Pleuni Hooijman<sup>1</sup>, Maria Falkenberg<sup>2</sup>, Mauro Modesti<sup>3</sup>, Erwin J.G. Peterman<sup>1</sup>, Gijs J.L. Wuite<sup>1</sup>.<sup>1</sup>VU University Amsterdam, Amsterdam, Netherlands, <sup>2</sup>Department of Medical Biochemistry and Cell Biology, Göteborg, Sweden, <sup>3</sup>Genome Instability and Carcinogenesis, Marseille, France.

Single-molecule manipulation techniques have provided a comprehensive understanding of the elastic behavior of DNA. We now know that its double-helical structure yields a significant persistence against bending on length scales of 150 base pairs and smaller. Interestingly, optical tweezers studies have also revealed, that at 65pN DNA undergoes a phase transition to another structure with significantly different elastic properties. Over a very narrow force range the polymer gains ~70% in contour length, and becomes significantly more flexible.

Until now the basic microscopic structure of overstretched DNA is under debate. Two qualitatively different models disagree on the molecular mechanism of the overstretching transition. The first one suggests that the DNA double helix unwinds to form a new structure, named S-DNA, which is usually depicted as a ladder with intact base pairing. The second model states that DNA overstretching is a force-induced melting transition, in which the hydrogen bonds between the two strands gradually break to yield single-stranded DNA, similar to thermal melting.

Using a combination of fluorescence microscopy and optical tweezers we directly visualize the DNA overstretching transition and demonstrate that it is driven by melting of the double-stranded DNA. In the experiments we use intercalating dyes and fluorescently labeled single-stranded binding proteins to specifically visualize double- and single-stranded segments in DNA molecules undergoing the transition. Our data unambiguously show that the overstretching transition comprises a gradual conversion from double-stranded to single-stranded DNA, in agreement with the force-induced melting model. Interestingly, not predicted by either model, we found that melting is nucleation-limited, typically initiating from DNA extremities and nicks.

**Platform J: Calcium Fluxes, Sparks, & Waves****106-Plat****Calcium Flickers Steer Cell Migration**Chaoliang Wei<sup>1</sup>, Xianhua Wang<sup>1</sup>, Min Chen<sup>1</sup>, Kunfu Ouyang<sup>1</sup>, Long-Sheng Song<sup>2</sup>, Heping Cheng<sup>1</sup>.<sup>1</sup>Institute of Molecular Medicine, National Laboratory of Biomembrane and Membrane Biotechnology, Peking University, Beijing, China, <sup>2</sup>Department of Internal Medicine, Division of Cardiovascular Medicine, University of Iowa Carver College of Medicine, Iowa, IA, USA.

Well-organized calcium signal in space, time and concentration is essential to directional movement, which is common to all cell types during development and critical to tissue remodeling and regeneration after damage. However, to date, it remains perplexing how calcium regulates the dynamics of leading lamella, which is the signalling and motility centre of a migrating cell, contains numerous effector proteins that require high levels of calcium for activation. Here we visualise, for the first time, high-calcium microdomains ("calcium flickers"), which are most active at the leading lamella of migrating fibroblasts, displaying a 4:1 front-to-rear polarisation opposite to the global calcium gradient (Fig). Calcium flicker activity is dually coupled to membrane tension (via TRPM7, a stretch-activated  $\text{Ca}^{2+}$ -permeant channel of the transient receptor potential superfamily) and chemoattractant signal transduction (via type 2 inositol 1,4,5-trisphosphate receptors). Interestingly, when exposed to a PDGF gradient perpendicular to cell movement, asymmetric calcium flicker activity develops across the lamella and promotes the turning of migrating fibroblasts. These findings illustrate how the exquisite spatiotemporal organisation of calcium microdomains can orchestrate complex cellular processes such as cell migration.

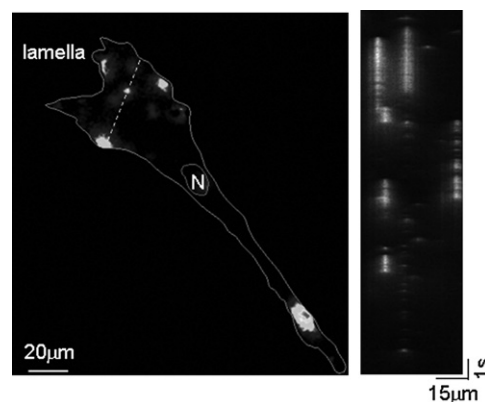


Figure: Calcium flickers in a migrating fibroblast.

**107-Plat** **$\text{Ca}^{2+}$  Spark Restitution In Ventricular Myocytes With Modified Ryanodine Receptor Gating**

Hena R. Ramay, Eric A. Sobie.

Mount Sinai School of Medicine, New York, NY, USA.

The local release of calcium ( $\text{Ca}^{2+}$ ) through sarcoplasmic reticulum ryanodine receptor channels (RyR) via  $\text{Ca}^{2+}$  induced  $\text{Ca}^{2+}$  release (CICR) is called a  $\text{Ca}^{2+}$  spark. The mechanisms responsible for the termination of  $\text{Ca}^{2+}$  sparks and refractoriness after termination remain a subject of debate. While local depletion of SR  $\text{Ca}^{2+}$  is clearly important for spark termination, the roles of SR refilling versus time-dependent changes in RyR gating in refractoriness and recovery are unclear. Using our previous experimental technique, here we further our findings by altering RyR gating behavior with caffeine and tetracaine. Isolated ventricular myocytes loaded with  $\text{Ca}^{2+}$  indicator fluo-3, were rapidly perfused with 50 nM of ryanodine together with either 100  $\mu\text{M}$  of caffeine, to sensitize RyRs, or 100  $\mu\text{M}$  tetracaine, to inhibit RyRs. At this very low concentration of ryanodine, limited number of RyR clusters have repetitive  $\text{Ca}^{2+}$  sparks. From confocal linescan images, we analyzed consecutive spark pairs from such clusters to measure  $\text{Ca}^{2+}$  spark amplitude and the triggering probability recovery. The recovery of  $\text{Ca}^{2+}$  spark amplitude was insensitive to altered RyR gating, with a time constant of recovery of ~70 ms in all three conditions. Modified RyR gating had a great impact on the distribution of spark-to-spark delays, however. The median delay between consecutive sparks was 169 ms for caffeine, 316 ms for control, and 371 ms for tetracaine. These results indicate that changes in RyR gating affect the recovery of  $\text{Ca}^{2+}$  spark triggering probability but not the recovery of  $\text{Ca}^{2+}$  spark amplitude. This strongly suggests that  $\text{Ca}^{2+}$  spark amplitude is determined primarily by the size of the local SR [ $\text{Ca}^{2+}$ ] store.

**108-Plat****Quarky Calcium Sparks in Heart**Didier X.P. Brochet<sup>1</sup>, Dongmei Yang<sup>2</sup>, Wenjun Xie<sup>3</sup>, Heping Cheng<sup>3</sup>, W.J. Lederer<sup>1</sup>.<sup>1</sup>University of Maryland Biotechnology Institute, Baltimore, MD, USA,<sup>2</sup>National Institute on Aging, National Institutes of Health, Baltimore, MD, USA, <sup>3</sup>Peking University, Beijing, China.

$\text{Ca}^{2+}$  sparks are the stereotyped unit of  $\text{Ca}^{2+}$  release in the heart and  $\text{Ca}^{2+}$  blinks are the reciprocal  $\text{Ca}^{2+}$  depletion signal produced in the exquisitely

small junctional sarcoplasmic reticulum (SR). With improved resolution and sensitivity that can be achieved by examining  $\text{Ca}^{2+}$  spark - blink pairs, we report here for the first time small, local but also sometimes spatially extensive  $\text{Ca}^{2+}$  releases (subsparks and  $\text{Ca}^{2+}$  "mist") that co-exist with regular  $\text{Ca}^{2+}$  sparks. Similar low-level  $\text{Ca}^{2+}$  releases also occur in the declining phase of regular  $\text{Ca}^{2+}$  sparks and the abundance of these small  $\text{Ca}^{2+}$  releases dictates the kinetics of the spark-blink pair. We propose a model in which the  $\text{Ca}^{2+}$  release unit, consisting of a large array of type 2 ryanodine receptor (RyR2)  $\text{Ca}^{2+}$  release channels, underlies the initial high-flux release of a  $\text{Ca}^{2+}$  sparks. In contrast, rogue unconstrained RyR2s, which may display higher  $\text{Ca}^{2+}$  sensitivity but smaller  $\text{Ca}^{2+}$  flux, produce the  $\text{Ca}^{2+}$  quark-like or "quarky" local releases. The existence of the additional release mechanism provides new fundamental mechanistic understanding of cardiac  $\text{Ca}^{2+}$  signaling in health and disease.

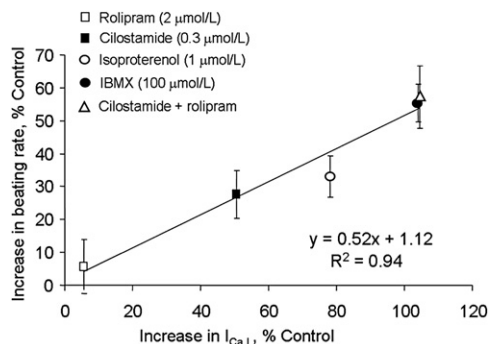
### 109-Plat

#### Concerted Phosphodiesterase (PDE) Subtype Activity Modulates $\text{Ca}^{2+}$ Influx Through L-type $\text{Ca}^{2+}$ Channels To Regulate Spontaneous Firing of Rabbit Sinoatrial Node Cells (SANC)

Tatiana M. Vinogradova, Alexey E. Lyashkov, Harold Spurgeon, Edward G. Lakatta.

NIA, NIH, Baltimore, MD, USA.

Spontaneous beating of rabbit SANC is controlled by cAMP-mediated, PKA-dependent rhythmic, local subsarcolemmal  $\text{Ca}^{2+}$  releases (LCRs) from sarcoplasmic reticulum during late diastolic depolarization. While  $\text{Ca}^{2+}$  influx via L-type  $\text{Ca}^{2+}$  channels ensures LCR occurrence, high basal PDE activity limits LCRs. The extent to which PDE regulates L-type  $\text{Ca}^{2+}$  current,  $I_{\text{Ca,L}}$ , however, remains enigma. We determined the extent of PDE subtype-dependent control of basal  $I_{\text{Ca,L}}$ , spontaneous SANC firing rate; and compared those to the effect of  $\beta$ -adrenergic receptor ( $\beta$ -AR) agonist, isoproterenol. A specific PDE4 inhibitor, rolipram, had no effect, on either  $I_{\text{Ca,L}}$  or spontaneous beating; cilostamide, a specific PDE3 inhibitor, in contrast, increased both  $I_{\text{Ca,L}}$  and spontaneous SANC firing (Fig). Simultaneous inhibition of PDE3 and PDE4 by (cilostamide + rolipram) increased  $I_{\text{Ca,L}}$ ; amplified LCR size (from  $5.9 \pm 0.58$  to  $8.6 \pm 0.50$   $\mu\text{m}$ ); decreased the LCR period (from  $309.7 \pm 20.6$  to  $214.3 \pm 3.9$  msec); and accelerated spontaneous SANC firing rate equivalent to broad-spectrum PDE inhibitor, IBMX. These effects were even greater than those produced by  $\beta$ -AR stimulation. Thus, concerted PDE3 and PDE4 activities control basal cAMP-PKA-dependent phosphorylation and suppress  $I_{\text{Ca,L}}$ , limiting basal LCRs and spontaneous SANC firing rate.



### 110-Plat

#### Development of Calcium Handling Defects During Aging in Spontaneously Hypertensive Rats

Sunil Kapur<sup>1</sup>, Gary L. Aistrup<sup>1</sup>, Rohan Sharma<sup>1</sup>, Jiabo Zheng<sup>1</sup>, James E. Kelly<sup>1</sup>, Alan H. Kadish<sup>1</sup>, William Balke<sup>2</sup>, J. Andrew Wasserstrom<sup>1</sup>.  
<sup>1</sup>Northwestern University, Chicago, IL, USA, <sup>2</sup>University of Kentucky, Lexington, KY, USA.

Several defects in calcium handling have been identified in failing myocytes. We investigated the progression of these defects in the course of development of overt heart failure (HF). Intracellular  $\text{Ca}^{2+}$  transients were measured using confocal microscopy in intact hearts from age-matched Wistar-Kyoto (WKY) control rats and Spontaneously Hypertensive Rats (SHR) at 6, 7.5, 9 and >22 months of age. Amplitude of basal  $\text{Ca}^{2+}$  transients (cycle length of 700msec) in SHR increased at 7.5 and 9 months, but subsequently decreased at 22 months compared to WKY. SHR myocytes exhibited longer transient duration starting at 9 months compared to WKY. Cell-to-cell variability in transient duration increased at 7.5 months and subsequently decreased at 9 months

as defects became more extensive. At 22 months,  $\text{Ca}^{2+}$  transients showed further increases in transient duration and intercellular variability. Restitution of  $\text{Ca}^{2+}$  release was slowed and was paralleled by increased  $\text{Ca}^{2+}$  alternans susceptibility starting at 9 months in SHR. Dyssynchronous alternans incidence increased beginning at 7.5 months in SHR compared to WKY. SHR myocytes also demonstrated an increased incidence of spontaneous  $\text{Ca}^{2+}$  waves at all ages, with the greatest difference at 22 months. A separate population of SHR myocytes showed  $\text{Ca}^{2+}$  waves that were activated during pacing ("triggered waves") whose incidence increased at all ages but most profoundly at 22 months. We conclude that well-coupled failing myocytes demonstrate progressively increasing defects in  $\text{Ca}^{2+}$  cycling. Biphasic changes in calcium transient magnitude may partially account for a transient inotropic effect during compensation but ultimately reduced cardiac output in HF. The progression of  $\text{Ca}^{2+}$  handling defects may also account for the increasing sensitivity to alternans as well as incidence of spontaneous and triggered  $\text{Ca}^{2+}$  waves with age, possibly explaining increased arrhythmias during progressive HF.

### 111-Plat

#### Decreased Arrhythmia Probability After Exercise Training In Post Infarction Heart Failure

Tomas O. Stølen<sup>1</sup>, Morten A. Høydal<sup>1</sup>, Godfrey L. Smith<sup>2</sup>, Ulrik Wisløff<sup>1</sup>.

<sup>1</sup>Norwegian University of Science and Technology, Trondheim, Norway,

<sup>2</sup>University of Glasgow, Glasgow, United Kingdom.

Background: Approximately half of all deaths in heart failure patients are attributed to sudden death or ventricular fibrillation (VF). Exercise training might protect against arrhythmias and VF, but the mechanism is not explored. The aim of this study was to measure how exercise training modulates VF in post myocardial infarction heart failure (HF) and further explore the cellular mechanisms.

Methods: We compared HF rats subjected to either moderate or high intensity exercise training with HF sedentary and sham. VF threshold and action potential duration (APD) were measured in isolated hearts, whereas  $\text{Ca}^{2+}$  cycling and SR  $\text{Ca}^{2+}$  leak were measured in Fura-2AM loaded cardiomyocytes. Additionally, t-tubule structure and  $\text{Ca}^{2+}$  release synchronicity were measured in single cardiomyocytes.

Results: VF occurred in 8/8 trials in the hearts from HF sedentary, 5/8 trials from HF exercise trained with moderate intensity, 1/9 trials in HF exercise trained with high intensity and 1/13 trials in sham. APD was increased in HF sedentary compared to sham ( $0.101 \pm 0.004$  ms vs.  $0.093 \pm 0.004$  ms, respectively). Moderate intensity exercise trained HF had normalized APD compared to sham while high intensity exercise training decreased APD to a level that was shorter than sham ( $0.085 \pm 0.007$  ms,  $P < 0.05$  vs. sham). Currently we are analyzing  $\text{Ca}^{2+}$  cycling including SR  $\text{Ca}^{2+}$  leak with and without CaMKII inhibitor and PKA inhibitor, AP, t-tubule structure and  $\text{Ca}^{2+}$  release synchronicity in single cardiomyocytes which will be finished before the meeting.

Conclusion: High intensity exercise training increase VF threshold and, thus decrease the incidence of ventricular fibrillation in heart failure.

### 112-Plat

#### $\text{Ca}^{2+}$ Spark Activity in Intact Dystrophin-Deficient mdx Muscle during Osmotic Challenge is Triggered by Mechanosensitive Pathways

Martin D.H. Teichmann<sup>1</sup>, Frederic von Wegner<sup>1</sup>, Rainer H.A. Fink<sup>1</sup>, Jeffrey S. Chamberlain<sup>2</sup>, Bradley S. Launikonis<sup>3</sup>, Boris Martinac<sup>3</sup>, Oliver Friedrich<sup>1,3</sup>.

<sup>1</sup>University of Heidelberg, Institute of Physiology/Pathophysiol, Heidelberg, Germany,

<sup>2</sup>University of Washington, Dept. Neurology, Seattle, WA, USA,

<sup>3</sup>University of Queensland, Brisbane, Australia.

Inhibitory DHPR control on RyR1 in intact dystrophic mdx skeletal muscle fibres was suggested to be disrupted, resulting in "uncontrolled"  $\text{Ca}^{2+}$  spark frequencies (CSF) during osmotic challenge (Wang et al., 2005, Nat. Cell. Biol.). However, some of their conditions must be considered completely unphysiologic (i.e. 50 mM external  $\text{Ca}^{2+}$ ). We recorded  $\text{Ca}^{2+}$  sparks in single intact wt, mdx and transgenic mini-dystrophin (MinD) expressing muscle fibres during hypo-/hypertonic challenge using confocal microscopy. CSF were low in wt and MinD, but twofold increased in mdx fibres under isotonic resting conditions. CSF increased faster during hypertonic than hypotonic challenge and peak CSF were about three times larger in mdx vs. wt and MinD fibres. CSF decayed exponentially ( $\tau_{\text{dec}}$ ) with ongoing challenge and were significantly faster in mdx fibres, thus questioning "uncontrolled" spark activity. In hypertonic solution, CSF  $\tau_{\text{dec}}$  was three times larger when external  $\text{Ca}^{2+}$  was 50 mM compared to 2 mM. Pretreatment with streptomycin or  $\text{Gd}^{3+}$  to block mechanosensitive channels (MsC), completely abolished the osmotic CSF increase mdx fibres. Resting membrane potentials in mdx muscle were  $\sim -61$  mV and  $\sim -73$  mV in wt fibres under hypertonic conditions (2 mM  $\text{Ca}^{2+}$ );